Pharmaceutical Sciences and Drug Design
ISSN: 3062-4428
2023, Volume 3, Page No: 138-156

Available online at: www.galaxypub.co/page/journals

Galaxy Publication

Ciprofol Mitigates Myocardial Ischemia/Reperfusion Injury by Suppressing Ferroptosis via HIF-1α Upregulation

Evelyn Mitchell[1]*, Caleb Parker[1]

[1]Department of Phytochemistry, Faculty of Life Sciences, University of Helsinki, Helsinki, Finland.

***E-mail** ✉ evelyn.mitch.fi@gmail.com

Received: 28 May 2023; **Revised:** 07 September 2023; **Accepted:** 08 September 2023

ABSTRACT

Ciprofol, a recently developed intravenous anesthetic, is increasingly utilized in anesthesia and sedation. While prior research has shown its potential to alleviate cerebral ischemia/reperfusion (I/R) injury by reducing oxidative stress and inflammation, its cardioprotective effects and underlying mechanisms remain unexplored. This study investigated whether ciprofol mitigates myocardial I/R injury by modulating ferroptosis. Myocardial I/R injury was induced in mice by 30 minutes of ischemia followed by 24 hours of reperfusion, and hypoxia/reoxygenation (H/R) injury was modeled in H9c2 cardiomyocytes with 6 hours of hypoxia and 6 hours of reoxygenation. Ciprofol was administered prior to ischemia or hypoxia. Assessments included echocardiography, TTC and HE staining, DAB-enhanced Perl's staining, transmission electron microscopy, and various assays for oxidative stress, mitochondrial function, and ferroptosis (FerroOrange, Liperfluo, JC-1, Rhodamine-123, DCFH-DA, Western blot). Cell viability, serum cardiac enzymes, and ferroptosis-related biomarkers were measured. HIF-1α was specifically targeted using siRNA and the inhibitor BAY87-2243 to explore the mechanistic basis.Administration of ciprofol markedly decreased infarct size and myocardial injury, reduced oxidative stress and mitochondrial damage, inhibited Fe^{2+} accumulation and ferroptosis, and improved cardiac performance in I/R-injured mice. Similarly, in H/R-treated cardiomyocytes, ciprofol enhanced cell survival, prevented mitochondrial dysfunction, and lowered intracellular Fe^{2+} and lipid peroxidation. Mechanistic studies revealed that ciprofol increased HIF-1α and GPX4 expression while suppressing ACSL4. The protective effects were reversed upon HIF-1α knockdown or inhibition, confirming its central role in ciprofol-mediated cardioprotection. Ciprofol exerts cardioprotective effects in myocardial I/R and H/R injury primarily by limiting ferroptosis through HIF-1α upregulation.

Keywords: GPX4/ACSL4, Myocardial ischemia/reperfusion injury, Ciprofol, HIF-1α, Ferroptosis, Oxidative stress

How to Cite This Article: Mitchell E, Parker C. Ciprofol Mitigates Myocardial Ischemia/Reperfusion Injury by Suppressing Ferroptosis via HIF-1α Upregulation. Pharm Sci Drug Des. 2023;3:138-56. https://doi.org/10.51847/5zXXEoIBES

Introduction

Myocardial infarction is a major contributor to cardiac arrest, particularly in middle-aged and elderly populations worldwide [1, 2]. While rapid restoration of blood flow to the ischemic myocardium is the cornerstone of treatment, reperfusion itself can paradoxically exacerbate tissue damage, a phenomenon known as ischemia/reperfusion (I/R) injury [3, 4]. Preserving cardiomyocyte survival is essential to maintain cardiac function following reperfusion therapy [5–7]. Despite extensive research into the molecular pathways involved, effective clinical strategies to prevent or limit myocardial I/R injury remain inadequate.

Ciprofol (HSK3486) is an innovative intravenous anesthetic developed as a structural derivative of propofol [8]. Clinically, it is employed for sedation and anesthesia during endoscopic procedures [9, 10], for induction and maintenance of general anesthesia [11], and for sedating critically ill patients under mechanical ventilation [12, 13]. Ciprofol offers sedative effects comparable to propofol while maintaining stable cardiovascular and respiratory parameters [14]. Although prior studies suggest that propofol can attenuate myocardial injury induced

by I/R or pharmacological stress [15, 16], whether ciprofol provides similar cardioprotective benefits—and the mechanisms through which it might do so—remain unclear.

Ferroptosis, a regulated cell death process marked by iron-dependent lipid peroxide accumulation, has been implicated in myocardial I/R injury [17–19]. Hypoxia-inducible factor-1α (HIF-1α) is a critical transcription factor that modulates ferroptosis, with its expression rising under hypoxic conditions to trigger protective signaling pathways that limit cellular damage [20–23]. Key molecular regulators of ferroptosis include glutathione peroxidase 4 (GPX4) and Acyl-CoA synthetase long-chain family member 4 (ACSL4) [20, 24]. This study aimed to explore whether ciprofol can prevent ferroptosis in the heart through HIF-1α activation, using both a mouse model of myocardial I/R injury and H9c2 cardiomyocytes subjected to hypoxia/reoxygenation (H/R).

Materials and Methods

Cell culture and Hypoxia/Reoxygenation (H/R) model

H9c2 cardiomyocytes (Cellverse Bioscience Technology Co., Ltd.) were maintained in Dulbecco's Modified Eagle Medium (DMEM) supplemented with 10% fetal bovine serum (FBS) and 1% penicillin/streptomycin at 37°C in a humidified incubator containing 5% CO_2. For H/R experiments, cells were switched to glucose-free medium (Procell, Wuhan, China) and exposed to a hypoxic atmosphere (95% N_2, 5% CO_2) for 6 hours, followed by 6 hours under normoxic conditions to allow reoxygenation.

In the first set of experiments, cells were treated with ciprofol at concentrations of 1, 5, 10, 50, and 100 μM under normal conditions (n = 5) to assess baseline effects. Subsequently, the same concentrations were applied prior to hypoxia (n = 5), and 10 μM was selected for further experiments. In the second set, cells were categorized into three groups: control, H/R, and H/R + ciprofol (n = 4–6). In the final set, HIF-1α expression was silenced using siRNA (si-HIF-1α) or negative control (si-NC), generating four groups: H/R, H/R + ciprofol, H/R + ciprofol + si-HIF-1α, and H/R + ciprofol + si-NC (n = 4–6). The overall experimental workflow is presented in **Figure 1a.**

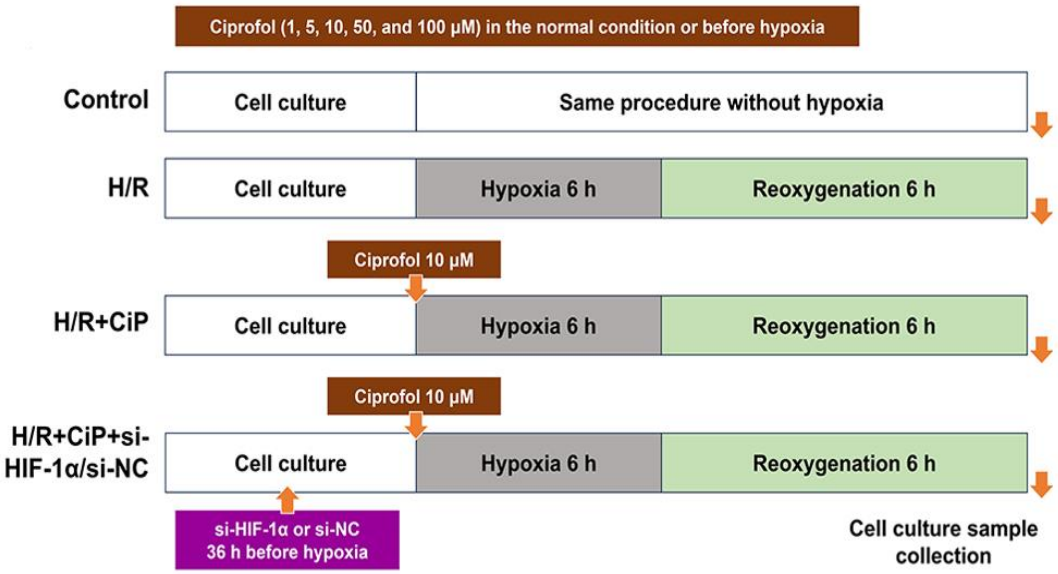

a)

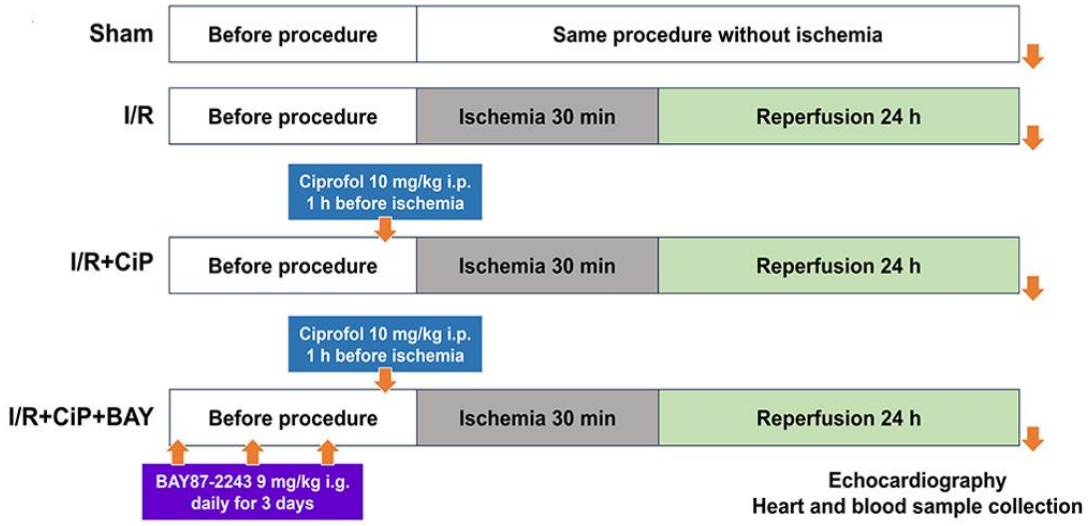

b)

Figure 1. Schematic Overview. (a) H9c2 cardiomyocytes were subjected to H/R injury. Initially, cells were treated with ciprofol at concentrations of 1, 5, 10, 50, and 100 μM under normal conditions or prior to hypoxia. Subsequently, a concentration of 10 μM ciprofol was used, and cells were transfected with si-HIF-1α or si-NC 36 hours before ciprofol administration. Cell samples were collected at the conclusion of reoxygenation. (b) In mice, myocardial I/R injury was induced. Ciprofol (10 mg/kg, i.p.) was administered one hour before ischemia, while BAY87-2243 (9 mg/kg, i.g.) was given daily for three consecutive days prior to ischemia. At the end of reperfusion, echocardiography was performed, and heart tissue and blood samples were collected.

Mouse myocardial I/R model

All animal procedures were approved by the Animal Ethics Committee of Soochow University (WDRM-20200713) and complied with the Guidelines for the Care and Use of Laboratory Animals. Male SPF-C57BL/6 mice (8–10 weeks old, 18–23 g) were obtained from Cavens Biogle Model Animal Research Co., Ltd. Mice were maintained under standard laboratory conditions (temperature 22–25°C, humidity 40–60%, 12-h light/dark cycle) with ad libitum access to food and water, and subjected to a 12-hour fasting period prior to experiments.

To establish myocardial I/R injury, mice were anesthetized with 1% sodium pentobarbital (50 mg/kg, i.p.), intubated, and mechanically ventilated. A small thoracotomy exposed the heart, and the left anterior descending coronary artery was ligated using 6–0 silk under a microscope. Successful ischemia was confirmed by blanching of the anterior left ventricle and ECG changes. After 30 minutes, the ligature was released to allow reperfusion, confirmed by restoration of anterior wall color and ST segment. Blood and heart tissues were collected after 24 hours of reperfusion.

Figure 1b illustrates the experimental design. Mice were randomized using a computer-generated list into three groups in part I (sham, I/R, I/R + ciprofol; n = 4–8) and four groups in part II (sham, I/R, I/R + ciprofol, I/R + ciprofol + BAY87-2243; n = 4–6). Sham animals underwent identical procedures without ligation. Mice in the I/R + ciprofol group received 10 mg/kg ciprofol (HSK3486, Haisco Pharmaceutical Group Co., Ltd., i.p.) one hour prior to ischemia. The I/R + ciprofol + BAY87-2243 group received BAY87-2243 (9 mg/kg, i.g.) daily for three days before ischemia; BAY87-2243 is a selective HIF-1α inhibitor [25, 26].

Cell transfection

siRNAs were synthesized by Guangzhou Ribo Biotechnology Co., Ltd. H9c2 cells were plated and cultured overnight, then transfected with vectors at a DNA:Lipomaster 2000 ratio of 1:3 (Novizan, Nanjing, China). After 6 hours, the medium was replaced, and cells were cultured for an additional 30 hours before further experimental treatments.

Echocardiography

Cardiac function was evaluated 24 hours post-reperfusion using transthoracic echocardiography (Vevo 2100, VisualSonics). Mice were anesthetized briefly with 2% sevoflurane. After applying ultrasound coupling gel, probe

positions were adjusted to obtain optimal long- and short-axis views of the left ventricle. Left ventricular end-diastolic and end-systolic diameters were measured to calculate ejection fraction (LVEF) and fractional shortening (LVFS). Each mouse was measured three times, and mean values were used.

Myocardial infarct assessment

Myocardial infarct size was determined using 2,3,5-triphenyltetrazolium chloride (TTC) staining. After reperfusion, the ligature was re-tightened at the original site, and Evans blue dye was injected via the tail vein. Hearts were excised, frozen for 30 minutes, sectioned, and stained with TTC for 20 minutes. Stained sections were imaged to quantify infarct area.

Histological analysis

Heart tissues were fixed in 4% paraformaldehyde for 24 hours, dehydrated, embedded in paraffin, and sectioned at 6 μm. Hematoxylin and eosin (HE) staining (Servicebio, Wuhan, China) was performed, and tissue morphology was imaged with an Olympus microscope.

DAB-enhanced perl's staining

Paraffin sections were deparaffinized, incubated in freshly prepared Perl's solution for 30 minutes, rinsed, and stained with DAB chromogen for 5 minutes. Nuclei were counterstained with hematoxylin for 1 minute, and brown iron deposition was visualized under a microscope.

Transmission electron microscopy

Myocardial tissue below the ligation site was cut into ~1 mm^3 sections, fixed in electron microscope fixative (G1102, Servicebio, Wuhan, China) for 2 hours at room temperature, then stored at 4°C for 24 hours. Ultra-thin sections were prepared and imaged using a transmission electron microscope.

Serum cardiac enzyme analysis

Blood samples collected post-reperfusion were centrifuged, and serum levels of CK-MB and cardiac troponin I (cTnI) were quantified using ELISA kits (Elabscience, USA) according to manufacturer instructions. Optical density values were recorded, and enzyme concentrations were calculated from standard curves.

Cell viability

H9c2 cell viability was measured with Cell Counting Kit-8 (CCK-8, APExBIO, TX, USA). Cells were plated in 96-well plates, and 10 μL of CCK-8 reagent was added per well post-treatment. After 2 hours of incubation in the dark, absorbance at 450 nm was recorded.

FerroOrange staining

Intracellular Fe^{2+} levels were assessed using FerroOrange (Maokang, Shanghai, China). Cells were incubated with 1 μM probe at 37°C for 30 minutes, followed by imaging under a microscope.

Liperfluo staining

To evaluate lipid peroxidation associated with ferroptosis, H9c2 cells were incubated with the Liperfluo probe (DOJINDO, L248, Japan). After H/R treatment and experimental interventions, cells were maintained in serum-free medium. Liperfluo working solution was added to achieve a final concentration of 5 μM, followed by incubation at 37°C for 30 minutes. Cells were then washed and imaged under a microscope.

Intracellular Reactive Oxygen Species (ROS) detection

Intracellular ROS levels were measured using the DCFH-DA fluorescent probe (Beyotime, Shanghai, China). At the end of treatments, DCFH-DA was added to serum-free DMEM at a final concentration of 1 μM and incubated in the dark for 30 minutes. Cells were washed with PBS, nuclei were counterstained with Hoechst 33342, and fluorescence images were captured.

Mitochondrial membrane potential assessment

Mitochondrial membrane potential was evaluated using Rhodamine-123 and JC-1 staining (Beyotime, Shanghai, China). Following treatment, cells were incubated with Rhodamine-123 or JC-1 working solutions in serum-free

DMEM at 1 μM for 30 minutes at 37°C in the dark. Excess dye was removed, and images were obtained with an inverted fluorescence microscope. In Rhodamine-123 staining, reduced green fluorescence indicates mitochondrial depolarization. For JC-1, an increase in green fluorescence accompanied by a reduction in red fluorescence reflects mitochondrial damage and loss of membrane potential.

Oxidative stress and ferroptosis biomarkers

Key markers of oxidative stress and ferroptosis—including LDH, SOD, lipid peroxidation (LPO), malondialdehyde (MDA), glutathione (GSH), and intracellular Fe^{2+}—were quantified. LDH levels rise following cellular damage, while SOD activity decreases. LPO and MDA are lipid peroxidation products, and GSH functions as an antioxidant; GSH levels decline during oxidative injury. Assays were performed according to the manufacturers' protocols using kits from Nanjing Jiancheng Bioengineering Institute (China), applied to both mouse heart tissue and cell culture supernatants.

Western blot analysis

Proteins were extracted from mouse hearts and H9c2 cells using RIPA lysis buffer (Beyotime, Shanghai, China), and concentrations were determined by BCA assay. Proteins were separated on 10% SDS-PAGE gels and transferred to PVDF membranes. Membranes were blocked with 5% skim milk for 2 hours at room temperature, then incubated overnight at 4°C with primary antibodies: HIF-1α (340462, Zenbio, China), ACSL4 (CY10198, Abways, China), GPX4 (CY6959, Abways, China), and GAPDH (FD0063, Fdbio Science, China). Following washing, membranes were incubated with HRP-conjugated secondary antibodies (1:4000, CoWin, China) for 2 hours at room temperature. Protein bands were visualized using enhanced chemiluminescence (New Cell Molecular Biotechnology, Suzhou, China) and quantified with ImageJ software.

Immunofluorescence staining

Mouse heart tissues were fixed in 4% paraformaldehyde for 24 hours, embedded in paraffin, and sectioned at 6 μm. After deparaffinization, antigens were retrieved using citric acid, and membranes were permeabilized with low-concentration Triton. Non-specific binding was blocked with donkey serum. Sections were incubated with primary HIF-1α antibody (340462, Zenbio, China), followed by fluorescent secondary antibody staining and DAPI nuclear counterstaining. Slides were mounted with antifade reagent and imaged using a fluorescence microscope. Signal intensity was analyzed using ImageJ software.

Statistical analysis

Data are expressed as mean ± standard deviation (SD). For groups with $n \geq 5$, one-way ANOVA with Dunnett's correction was used for multiple comparisons. Smaller groups ($n < 5$) were analyzed using permutation tests. Analyses were performed with GraphPad Prism 9 (GraphPad, San Diego, CA, USA) and R (version 3.6.0, R Foundation, Vienna, Austria). P values < 0.05 were considered statistically significant.

Results and Discussion

Ciprofol attenuates H/R-induced oxidative damage in H9c2 cells

Cell viability of H9c2 cardiomyocytes was first examined after treatment with ciprofol at 1, 5, 10, 50, and 100 μM under normal conditions and following H/R **(Figures 2a and 2b)**. Ciprofol at 10 μM provided the greatest protective effect. Higher concentrations (50 and 100 μM) decreased cell viability under normal conditions and did not rescue H/R-induced cell injury. Therefore, 10 μM was used in all subsequent experiments.

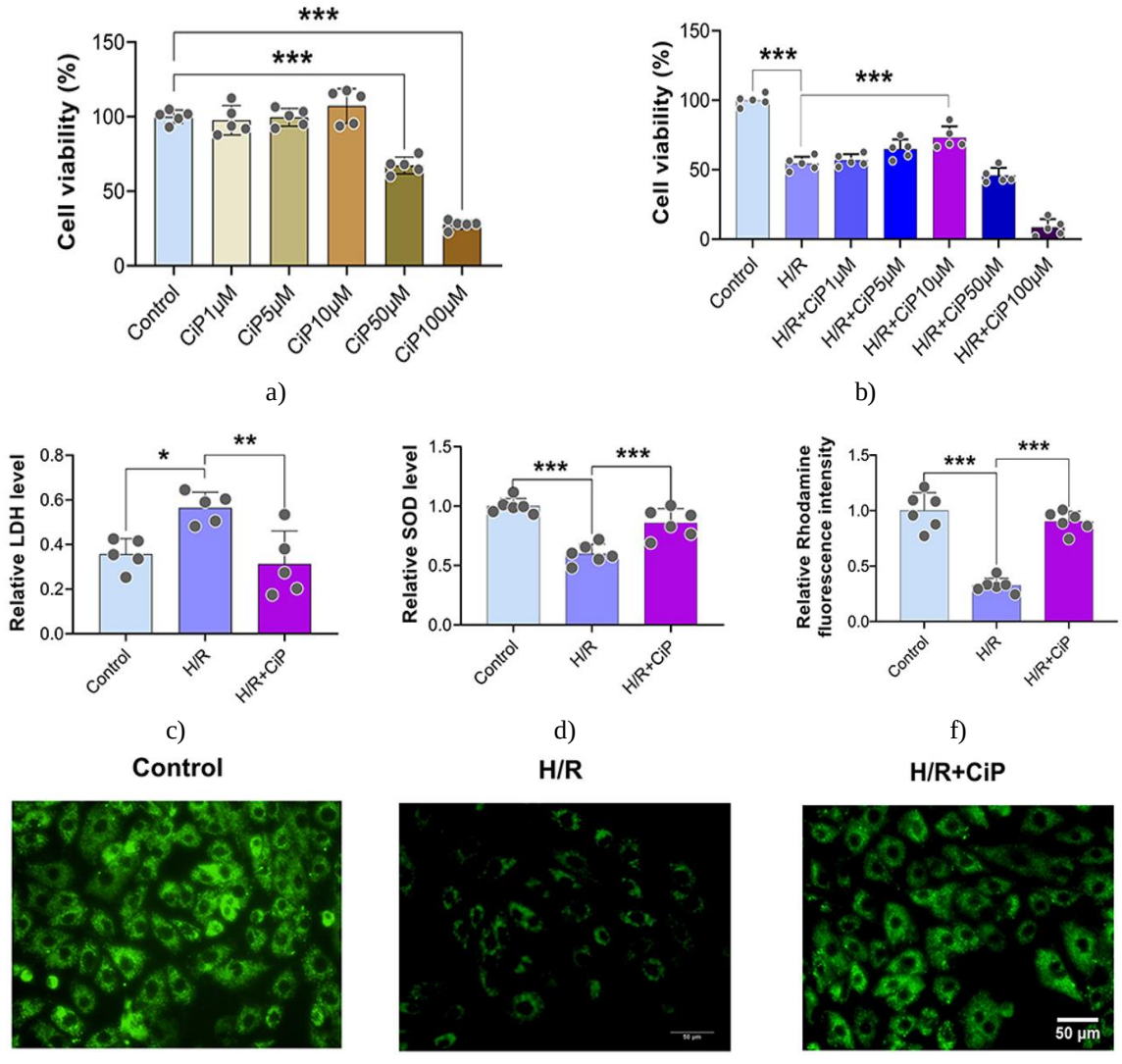

Figure 2. Ciprofol Mitigates H/R-Induced Injury in H9c2 Cardiomyocytes. (a) Viability of H9c2 cells treated with ciprofol (1, 5, 10, 50, and 100 μM) under normal conditions. (b) Cell viability following H/R with the same ciprofol concentrations. (c, d) Levels of LDH and SOD in culture supernatants. Ciprofol (10 μM) was administered 1 hour prior to H/R. (e, f) Representative images and quantification of Rhodamine-123 staining for mitochondrial membrane potential. Ciprofol (10 μM) was applied 1 hour before H/R. Scale bar = 50 μm. Data are expressed as mean ± SD (n = 5–6). *P < 0.05, **P < 0.01, ***P < 0.001.

Exposure to H/R markedly elevated LDH release and decreased SOD activity in the culture medium, reflecting pronounced oxidative injury. Pretreatment with ciprofol significantly mitigated these changes, suggesting attenuation of H/R-induced oxidative stress **(Figures 2c and 2d)**. Furthermore, Rhodamine-123 staining revealed that H/R led to mitochondrial membrane depolarization, which was substantially prevented by ciprofol, indicating preservation of mitochondrial integrity **(Figures 2e and 2f).**

Ciprofol reduces oxidative stress and myocardial I/R damage in vivo

In mice subjected to myocardial I/R, TTC staining demonstrated that pretreatment with ciprofol decreased the infarcted area relative to untreated I/R controls **(Figure 3a and 3b).** Histological examination with HE staining showed that ciprofol alleviated structural damage in myocardial tissue caused by I/R injury **(Figure 3c).** Additionally, serum assays revealed that levels of CK-MB and cTnI were significantly lower in the ciprofol-treated group, indicating reduced cardiomyocyte injury **(Figures 3d and 3e).**

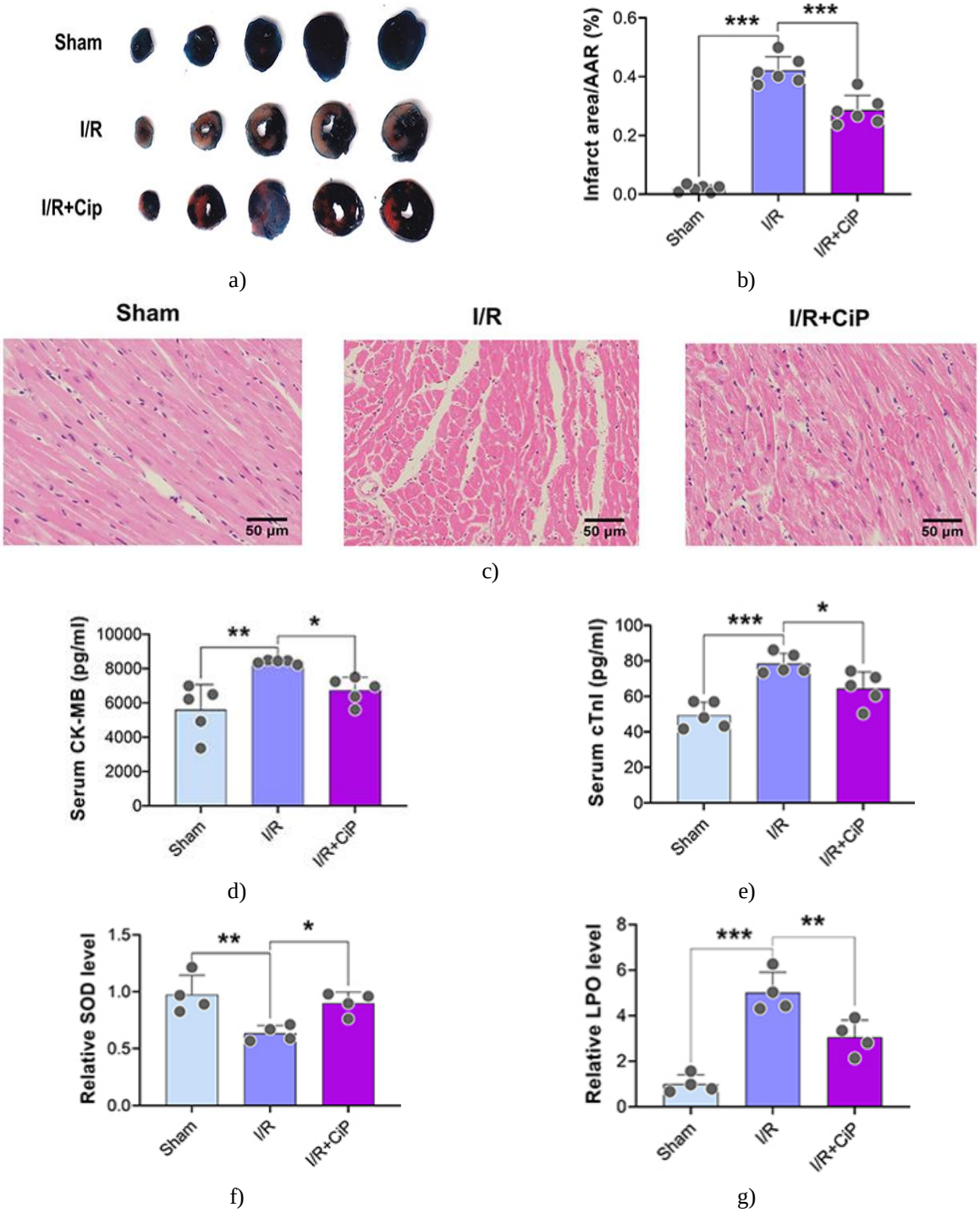

Figure 3. Ciprofol Reduces Myocardial I/R Injury in Mice. Mice received ciprofol (10 mg/kg, i.p.) one hour prior to ischemia. (a, b) Representative TTC-stained heart sections and quantitative analysis of infarct size. (c) Representative HE-stained myocardial tissue images. Scale bar = 50 μm. (d, e) Serum levels of cardiac injury markers CK-MB and cTnI. (f, g) Serum antioxidant and lipid peroxidation markers, SOD and LPO. Data are presented as mean ± SD (n = 4–6). *P < 0.05, **P < 0.01, ***P < 0.001.

Myocardial I/R injury caused a marked reduction in serum SOD levels along with an increase in LPO, indicating oxidative stress, whereas pretreatment with ciprofol effectively restored SOD and lowered LPO, demonstrating cardioprotection against oxidative damage **(Figures 3f and 3g).**

Echocardiographic assessment further revealed that ciprofol significantly enhanced cardiac performance. Mice treated with ciprofol exhibited higher left ventricular ejection fraction (LVEF) and fractional shortening (LVFS) compared to untreated I/R mice, indicating improved myocardial function **(Figures 4a–4c).**

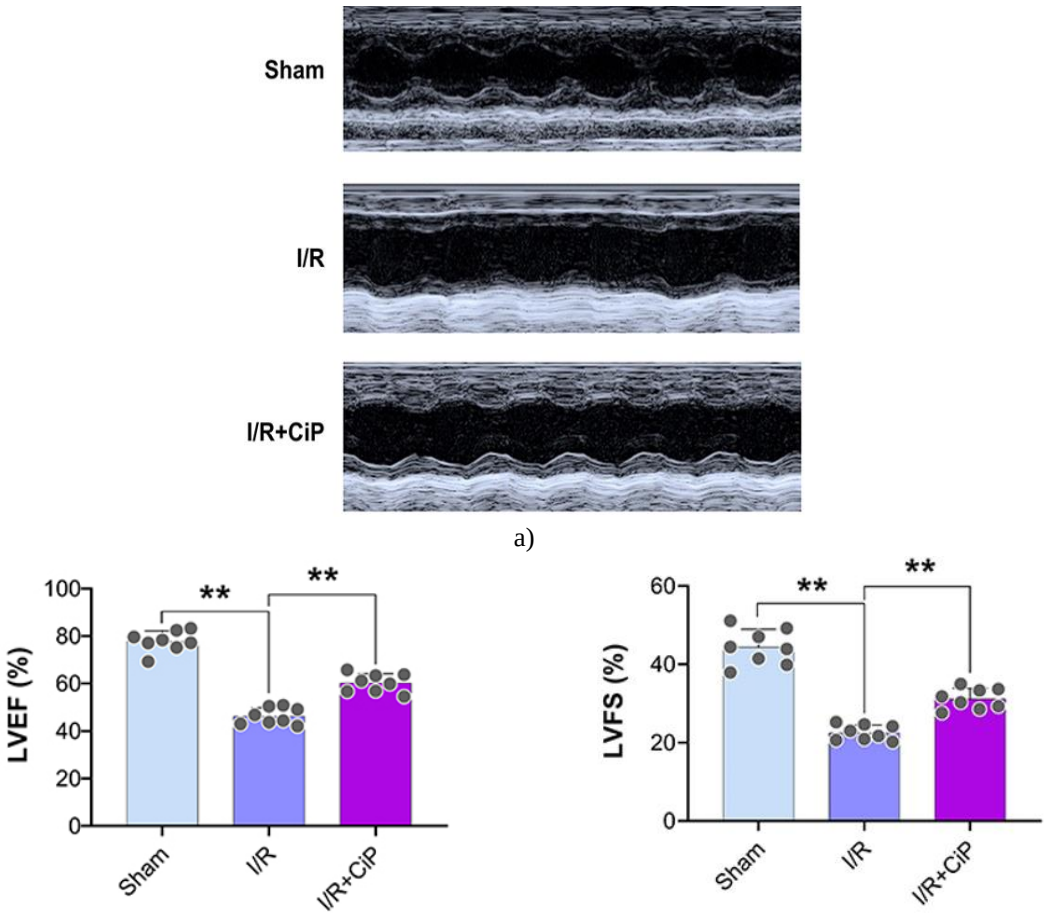

Figure 4. Ciprofol Enhances Cardiac Function in Mice Following Myocardial I/R. Mice were pretreated with ciprofol (10 mg/kg, i.p.) one hour before ischemia. (a) Representative echocardiographic images. (b, c) Quantitative measurements of LVEF and LVFS. Data are expressed as mean ± SD (n = 8). **P < 0.01.

Ciprofol attenuates ferroptosis and upregulates HIF-1α in H/R-treated cardiomyocytes

FerroOrange staining demonstrated that ciprofol markedly reduced intracellular Fe^{2+} accumulation in H9c2 cells compared with the H/R group, indicating suppression of iron-dependent oxidative damage **(Figures 5a and 5b).** Liperfluo staining further revealed that ciprofol significantly decreased intracellular lipid peroxidation caused by H/R injury **(Figures 5c and 5d).** Consistently, ciprofol treatment lowered cellular Fe^{2+} and malondialdehyde (MDA) levels, confirming its protective effect against ferroptosis **(Figures 5e and 5f).**

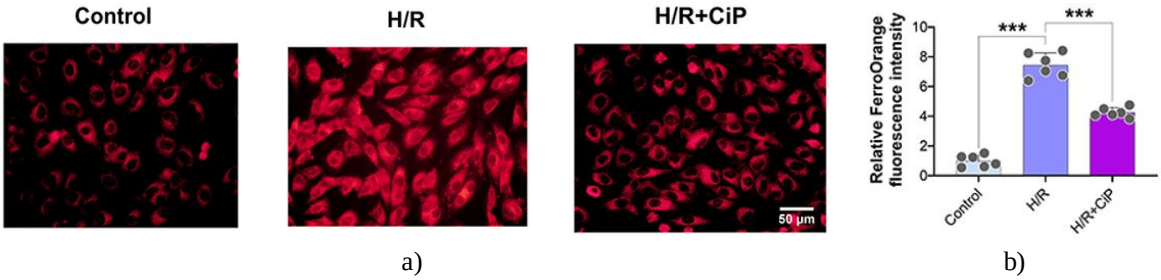

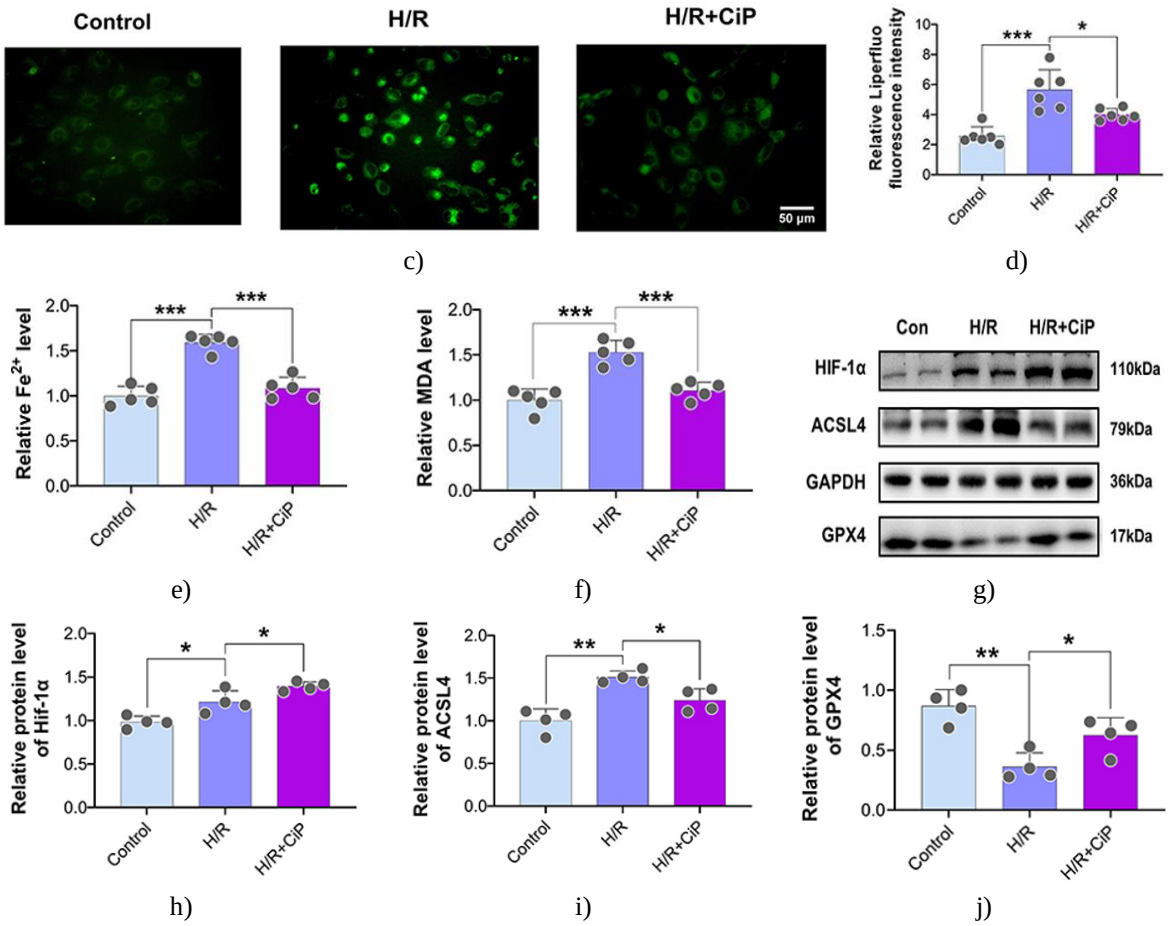

Figure 5. Ciprofol Suppresses Ferroptosis and Enhances HIF-1α in H9c2 Cardiomyocytes During H/R

Cells were treated with ciprofol (10 μM) 1 hour prior to H/R. (A, B) Representative FerroOrange staining images and corresponding fluorescence quantification. Scale bar = 50 μm. (C, D) Representative Liperfluo staining images and fluorescence intensity analysis. Scale bar = 50 μm. (E, F) Intracellular levels of Fe^{2+} and MDA. (G–J) Western blot analysis and quantification of HIF-1α, ACSL4, and GPX4 protein expression. Data are shown as mean ± SD (n = 4–6). *P < 0.05, **P < 0.01, ***P < 0.001.

Western blot analysis revealed that H/R injury induced an upregulation of HIF-1α and ACSL4 while reducing GPX4 expression **(Figures 5g–5j)**. Treatment with ciprofol further enhanced HIF-1α levels and partially reversed the H/R-mediated alterations in ACSL4 and GPX4, indicating inhibition of ferroptosis.

Ciprofol reduces myocardial I/R-induced Fe^{2+} overload and mitochondrial injury in mice

To examine whether ciprofol mitigates iron accumulation in the myocardium, Perl's staining was performed. Myocardial I/R led to pronounced Fe^{2+} deposition, which was markedly reduced by pretreatment with ciprofol **(Figure 6a)**, suggesting protection against iron-mediated oxidative damage.

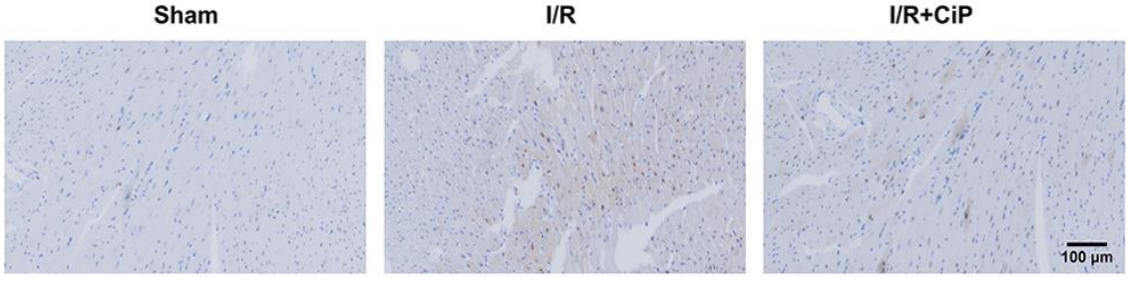

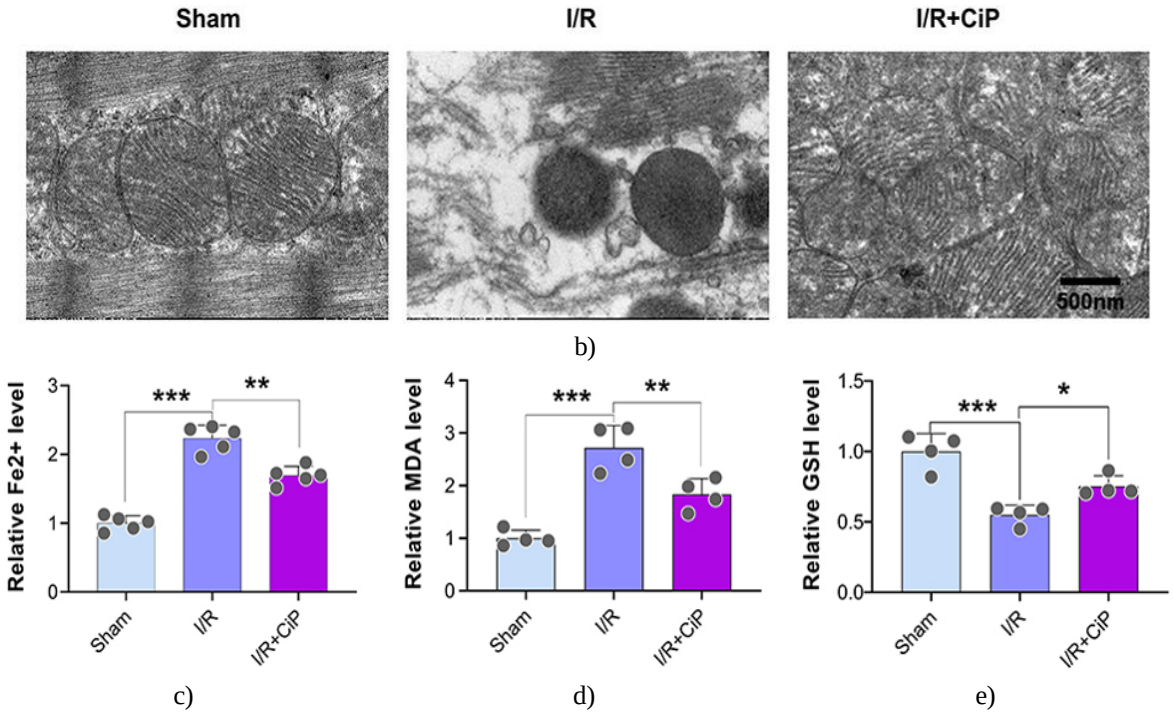

Figure 6. Ciprofol Mitigates Fe^{2+} Overload and Mitochondrial Injury in Mice with Myocardial I/R

Mice were pretreated with ciprofol (10 mg/kg, i.p.) 1 hour before ischemia. (A) Representative images of myocardial Perl's staining. Scale bar = 100 μm. (B) Mitochondrial ultrastructure visualized by transmission electron microscopy. Scale bar = 500 nm. (C–E) Serum levels of Fe^{2+}, MDA, and GSH. Data are expressed as mean ± SD (n = 4–5). *P < 0.05, **P < 0.01, ***P < 0.001.

Transmission electron microscopy revealed that myocardial I/R caused mitochondria to exhibit condensed morphology and disrupted cristae, whereas ciprofol treatment preserved mitochondrial structure **(Figure 6b).** Measurements of ferroptosis-related biomarkers showed that ciprofol suppressed the accumulation of Fe^{2+} and MDA while restoring GSH levels in the myocardium, indicating effective inhibition of ferroptotic damage during I/R injury **(Figures 6c–6e).**

Ciprofol attenuates H/R-induced ferroptosis in cardiomyocytes via HIF-1α upregulation

To investigate the involvement of HIF-1α in ciprofol-mediated cardioprotection, HIF-1α expression was silenced using siRNA in H9c2 cells. Ciprofol treatment reduced LDH and LPO release and increased SOD activity in H/R-exposed cells; however, knockdown of HIF-1α reversed these protective effects, confirming the role of HIF-1α in mediating ciprofol's inhibition of oxidative stress and ferroptosis **(Figures 7a–7c).**

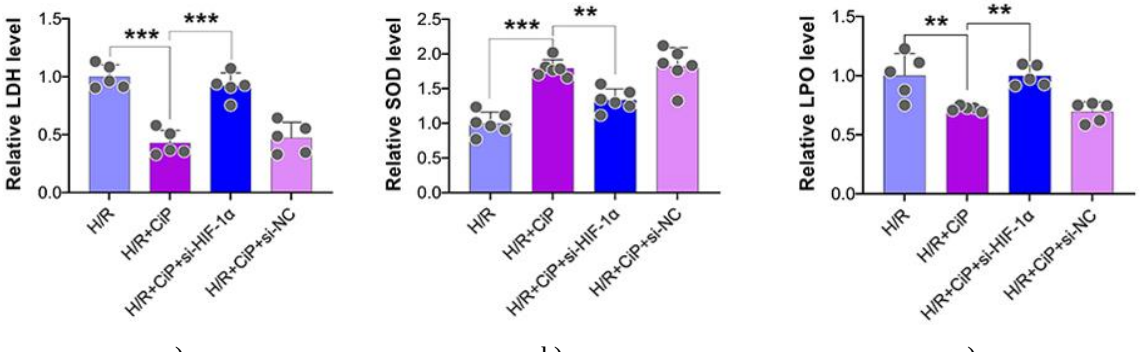

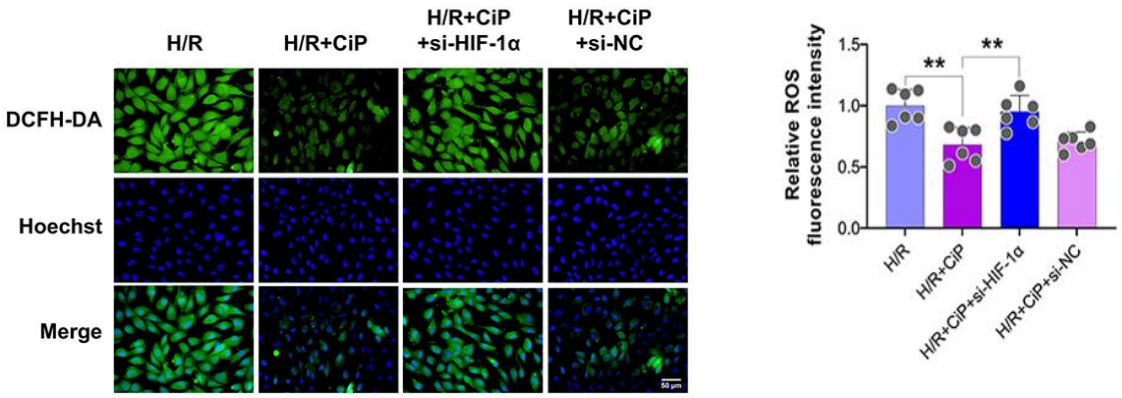

d) e)

Figure 7. Silencing HIF-1α Abolishes Ciprofol's Protective Effects Against H/R Injury in H9c2 Cardiomyocytes

H9c2 cells were transfected with si-HIF-1α or si-NC 36 hours prior to treatment with ciprofol (10 μM). (A–C) Levels of LDH, SOD, and LPO in the different groups. (D, E) Representative DCFH-DA staining images and quantification of intracellular ROS. Scale bar = 50 μm. Data are presented as mean ± SD (n = 5–6). **P < 0.01, ***P < 0.001.

DCFH-DA staining indicated that ciprofol significantly reduced intracellular ROS accumulation during H/R injury, whereas knockdown of HIF-1α markedly increased ROS levels, counteracting ciprofol's effect **(Figures 7d and 7e).**

Mitochondrial membrane potential was evaluated using the JC-1 probe. Ciprofol decreased JC-1 monomer (green) fluorescence while enhancing JC-1 aggregate (red) fluorescence, indicating preservation of mitochondrial function under H/R stress **(Figures 8a–8c)**. Silencing HIF-1α reversed these benefits, confirming that ciprofol's mitochondrial protective effects depend on HIF-1α signaling.

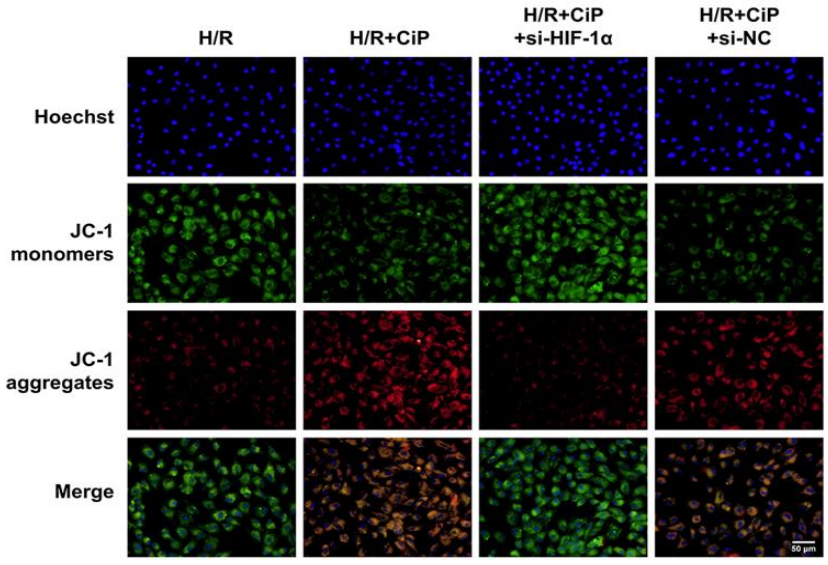

a)

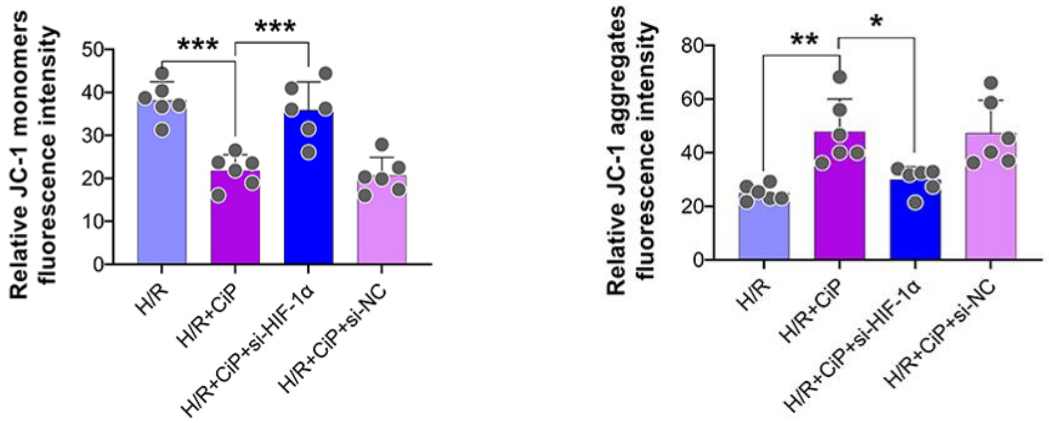

b) c)

Figure 8. HIF-1α Knockdown Abrogates Ciprofol-Mediated Protection of Mitochondrial Function in H9c2 Cells Under H/R

H9c2 cardiomyocytes were transfected with si-HIF-1α or si-NC 36 hours prior to treatment with ciprofol (10 μM). (A) Representative JC-1 staining images indicating mitochondrial membrane potential. Scale bar = 50 μm. (B, C) Quantification of JC-1 monomers (green) and aggregates (red). Data are presented as mean ± SD (n = 6). *P < 0.05, **P < 0.01, ***P < 0.001.

Ciprofol treatment during H/R injury decreased intracellular Fe^{2+} and MDA levels while elevating GSH content, effects that were partially reversed by HIF-1α silencing **(Figures 9a–9c)**. Knockdown of HIF-1α resulted in a pronounced increase in Fe^{2+} accumulation, as shown by FerroOrange staining **(Figures 9d and 9e)**, and enhanced intracellular lipid peroxidation, detected using Liperfluo staining **(Figures 9f and 9g),** indicating that HIF-1α is critical for ciprofol-mediated inhibition of ferroptosis.

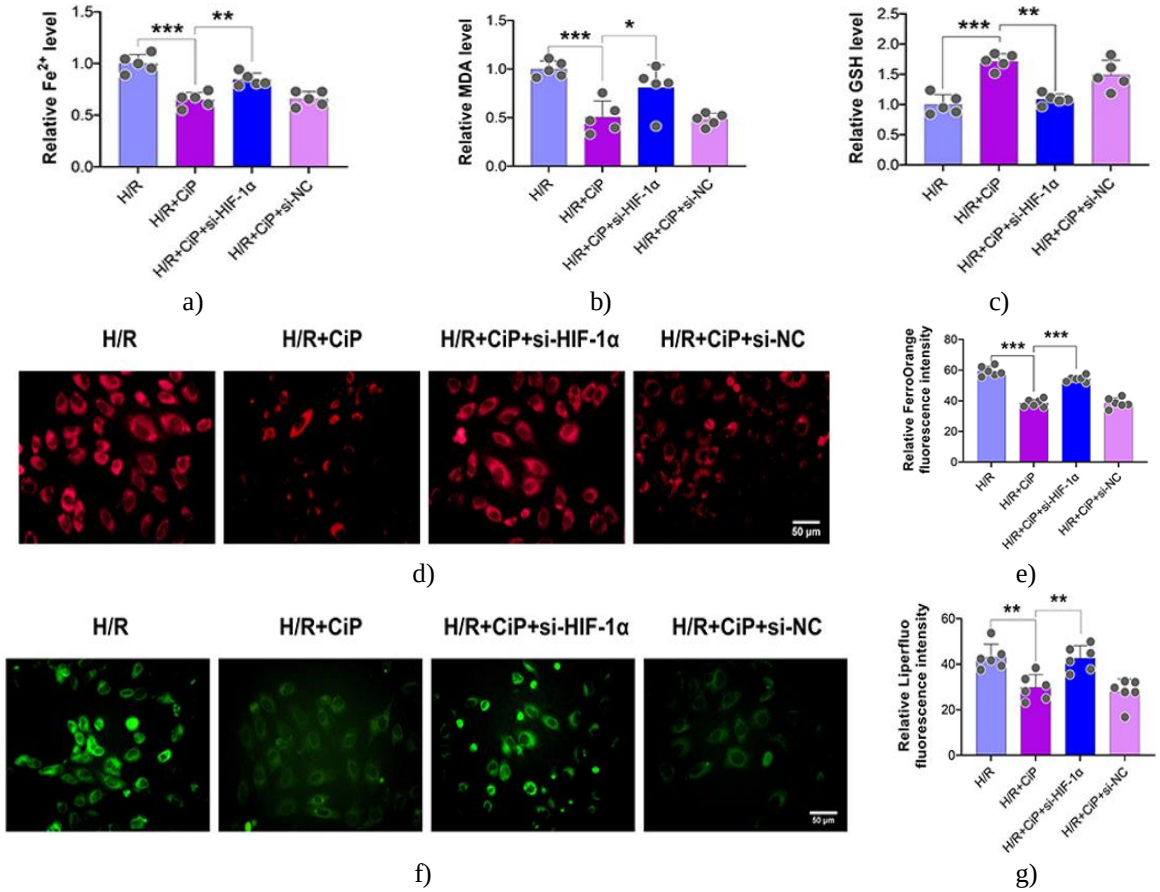

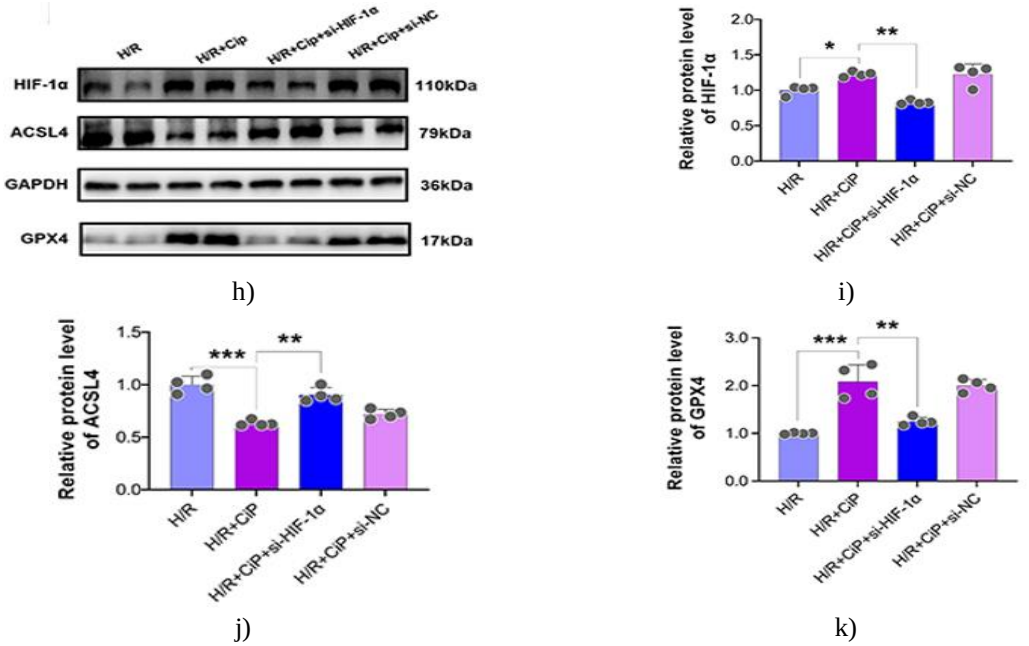

Figure 9. Ciprofol Attenuates H/R-Induced Ferroptosis in H9c2 Cardiomyocytes via HIF-1α Upregulation

H9c2 cells were transfected with si-HIF-1α or si-NC 36 hours prior to treatment with ciprofol (10 μM). (A–C) Levels of Fe^{2+}, MDA, and GSH. (D, E) Representative images and quantification of FerroOrange staining. Scale bar = 50 μm. (F, G) Representative images and fluorescence intensity of Liperfluo staining. Scale bar = 50 μm. (H–K) Western blot analysis and quantification of HIF-1α, ACSL4, and GPX4 expression. Data are presented as mean ± SD (n = 4–6). *P < 0.05, **P < 0.01, ***P < 0.001.

Western blot analysis revealed that ciprofol treatment elevated HIF-1α and GPX4 protein levels while suppressing ACSL4 expression in H/R-exposed cells, whereas silencing HIF-1α negated these effects, confirming that ciprofol inhibits ferroptosis through HIF-1α signaling **(Figures 9h–9k).**

Ciprofol protects against myocardial I/R injury and ferroptosis in mice via HIF-1α activation

TTC staining demonstrated that inhibition of HIF-1α by BAY87-2243 abolished the protective effect of ciprofol on myocardial infarction in mice subjected to I/R injury **(Figures 10a and 10b)**. Analysis of ferroptosis markers in the myocardium showed that ciprofol decreased Fe^{2+} accumulation and restored GSH levels, whereas these benefits were reversed upon treatment with the HIF-1α inhibitor **(Figures 11a and 11b)**. Additionally, Perl's staining confirmed that ciprofol reduced Fe^{2+} deposition in myocardial tissue during I/R, an effect blocked by BAY87-2243 **(Figure 11c),** highlighting the essential role of HIF-1α in mediating ciprofol's cardioprotective actions.

Figure 10. HIF-1α Inhibition Abolishes Ciprofol's Protective Effect on Myocardial I/R Injury in Mice Mice received BAY87-2243 (9 mg/kg, i.g.) daily for 3 consecutive days before ischemia to inhibit HIF-1α. (a) Representative images of myocardial TTC staining. (b) Quantification of infarct size. Data are expressed as mean ± SD (n = 6). **P < 0.01, ***P < 0.001.

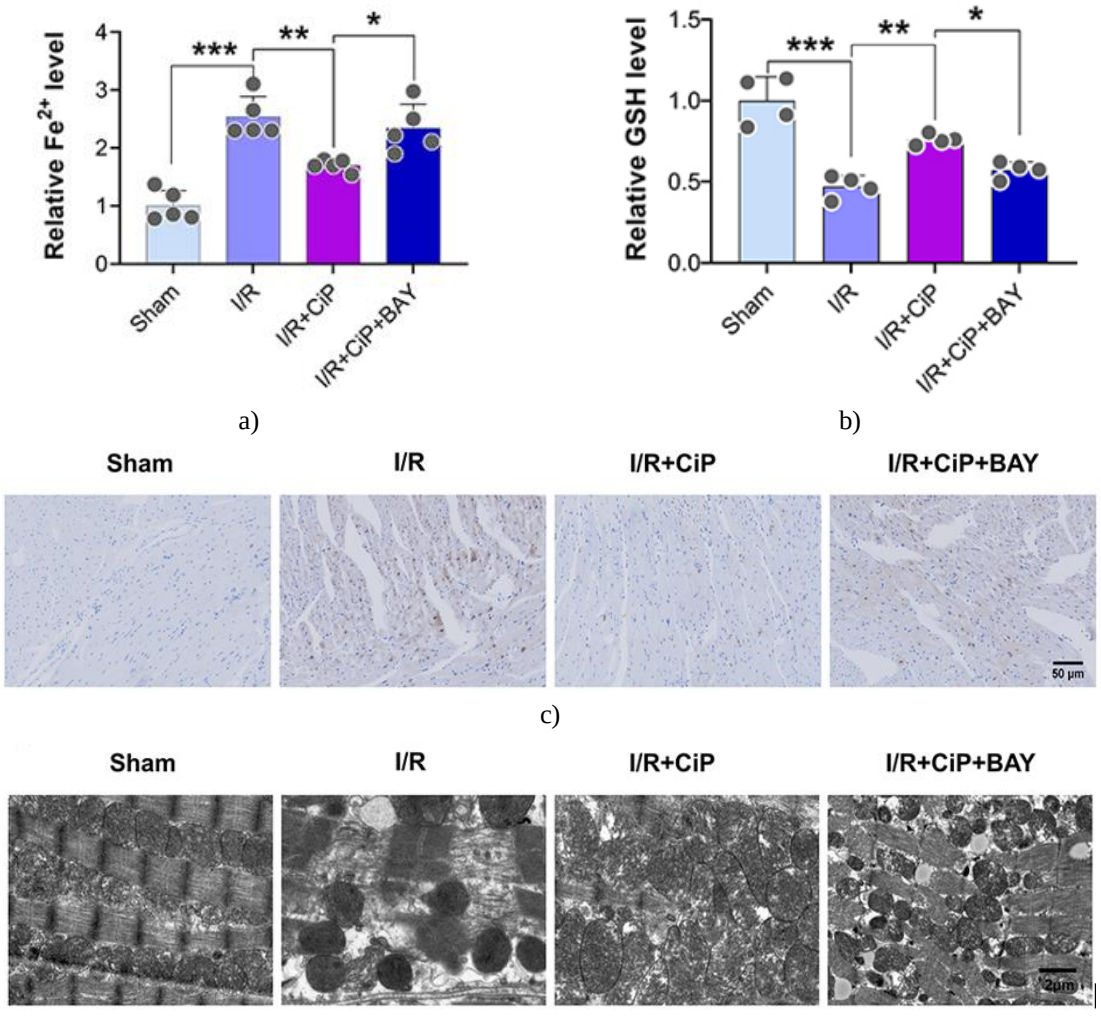

Figure 11. HIF-1α Inhibition Abrogates Ciprofol's Protective Effects on Fe^{2+} Accumulation and Mitochondrial Integrity in Mice With Myocardial I/R Injury

Mice were treated with BAY87-2243 (9 mg/kg, i.g.) daily for 3 days prior to ischemia. (A, B) Serum Fe^{2+} and GSH levels. (C) Representative Perl's staining of myocardial tissue. Scale bar = 50 μm. (D) Representative transmission electron microscopy images of mitochondrial ultrastructure. Scale bar = 2 μm. Data are presented as mean ± SD (n = 4–5). *P < 0.05, **P < 0.01, ***P < 0.001.

Transmission electron microscopy revealed that ciprofol alleviated the mitochondrial damage induced by myocardial I/R, whereas HIF-1α inhibition abolished this protective effect **(Figure 11d).** Immunostaining further showed that myocardial I/R injury increased HIF-1α expression, which was further enhanced by ciprofol, but BAY87-2243 significantly reduced HIF-1α levels **(Figures 12a and 12b).** Consistently, Western blot analysis confirmed that ciprofol upregulated HIF-1α and GPX4 while downregulating ACSL4 in I/R-injured hearts, and inhibition of HIF-1α reversed these effects **(Figures 12c–12f),** demonstrating the central role of HIF-1α in mediating ciprofol's cardioprotective and anti-ferroptotic actions.

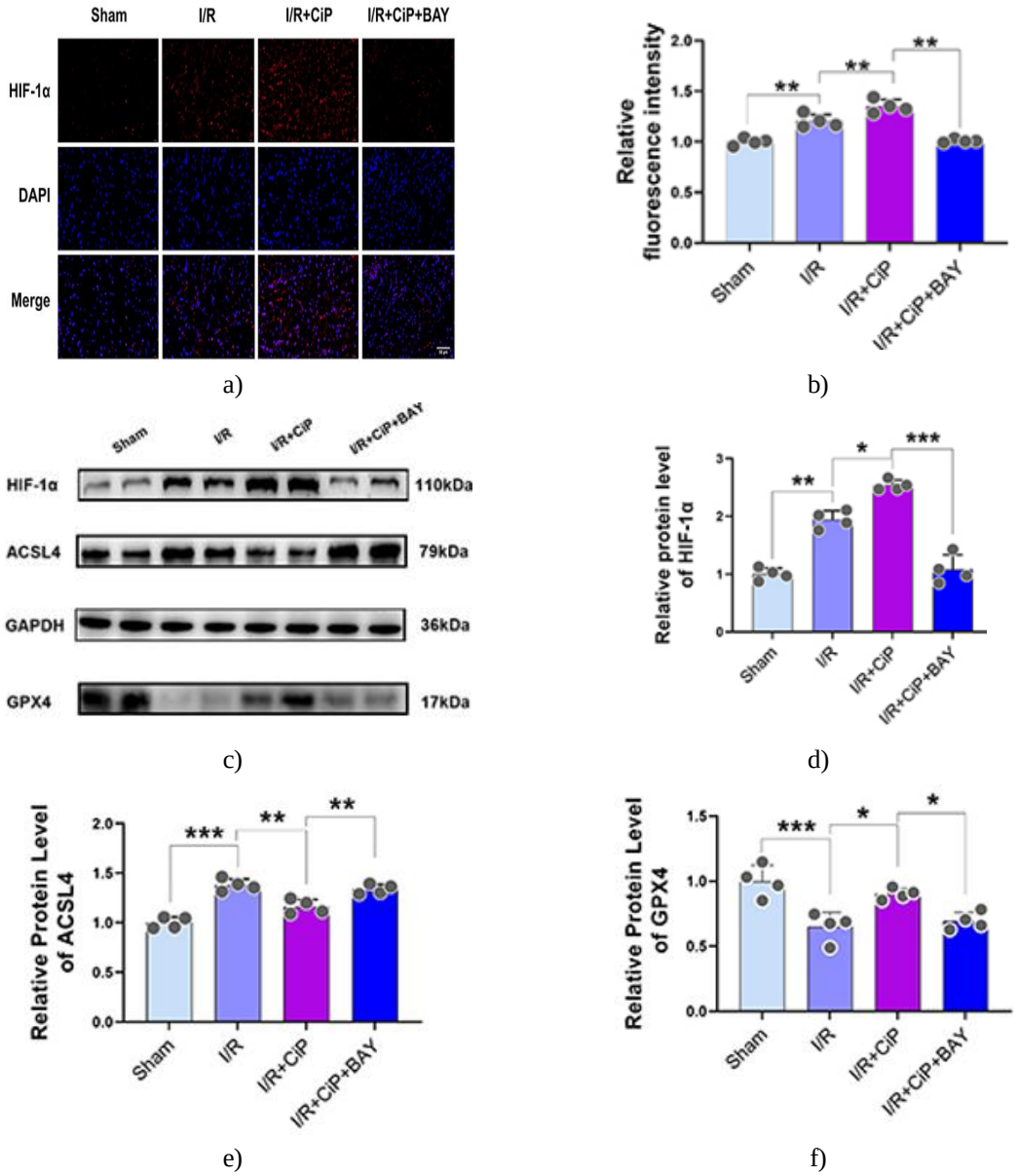

Figure 12. Ciprofol Mitigates Myocardial Ferroptosis in Mice Through HIF-1α Upregulation

BAY87-2243 (9 mg/kg, i.g.) was administered daily for 3 days prior to ischemia. (A, B) Representative immunofluorescence images and quantification of HIF-1α expression in myocardial tissue. Scale bar = 50 μm. (C–F) Western blot images and quantification of HIF-1α, ACSL4, and GPX4 protein levels. Data are expressed as mean ± SD (n = 4). *P < 0.05, **P < 0.01, ***P < 0.001.

In the present study, both in vivo and in vitro experiments revealed that pretreatment with ciprofol significantly alleviated myocardial I/R injury in mice and reduced H/R-induced damage in H9c2 cardiomyocytes. The cardioprotective effects of ciprofol were mainly mediated through the suppression of ferroptosis by upregulating HIF-1α and modulating the downstream GPX4/ACSL4 pathway.

Ferroptosis, a unique form of regulated cell death driven by iron-dependent lipid peroxidation, plays a critical role during reperfusion and contributes substantially to myocardial injury [18, 19, 27, 28]. Previous research demonstrated that inhibition of ferroptosis protects the heart against I/R damage. Propofol has been reported to mitigate ferroptosis by maintaining mitochondrial integrity and regulating iron homeostasis and antioxidant enzymes [29]. In line with these findings, our results indicate that ciprofol decreased iron deposition, suppressed lipid peroxide formation, and preserved mitochondrial structure following I/R or H/R injury.

HIF-1α, a hypoxia-inducible transcription factor, is known to protect the myocardium under hypoxic conditions [30]. Our study showed that ciprofol enhanced HIF-1α expression, whereas silencing HIF-1α via siRNA or inhibiting it with BAY87-2243 increased ferroptosis and aggravated myocardial damage. These findings are

consistent with previous studies demonstrating that HIF-1α activation inhibits ferroptotic death in cardiomyocytes and neurons [31, 32]. We also observed that HIF-1α modulates GPX4 and ACSL4 expression, suggesting that the GPX4/ACSL4 pathway functions downstream of HIF-1α in mediating ferroptosis in our experimental models.

Ciprofol is a novel intravenous anesthetic derived from propofol, exhibiting higher anesthetic potency, reduced injection-associated pain, and a favorable safety profile [33, 34]. Dose adjustments are unnecessary in patients with mild-to-moderate renal impairment [35]. Ciprofol has demonstrated neuroprotective effects against cerebral I/R injury in mice [36], and prior studies suggested it may also attenuate myocardial injury, though mechanisms were unclear [37]. Our study confirmed that ciprofol reduced serum CK-MB and cTnI levels and improved cardiac function in mice following I/R injury, highlighting its potential clinical advantage for perioperative cardiac protection [38].

Based on body surface area calculations for dose conversion from mice to humans [39, 40], the mouse dose of 10 mg/kg corresponds to approximately 0.81 mg/kg in humans, which aligns with clinical anesthesia doses (0.4 mg/kg induction, 0.8–2.4 mg/kg/h maintenance) [14, 34]. In vitro, 10 μM ciprofol effectively protected cardiomyocytes from H/R injury, while higher concentrations (50–100 μM) reduced cell viability, indicating potential cytotoxicity at elevated doses.

Our findings provide a mechanistic rationale for using ciprofol during anesthesia in patients at high risk of myocardial I/R injury, such as those with ischemic heart disease or undergoing cardiac surgery. While ciprofol is not intended as a primary therapy for cardiovascular disease, its use during anesthesia may mitigate perioperative myocardial damage. However, translation to clinical practice requires further trials.

This study has several limitations. We used H9c2 cells instead of primary neonatal cardiomyocytes, although in vivo experiments in mice complemented these findings. While we demonstrated that ciprofol inhibited ferroptosis via HIF-1α and the GPX4/ACSL4 pathway, the precise mechanism by which ciprofol regulates HIF-1α remains to be clarified. Other forms of cell death, including apoptosis and necrosis, may also contribute to myocardial I/R injury. Some groups had small sample sizes (n = 4), and permutation tests were employed to ensure robust statistical analysis. Finally, whether ciprofol offers superior cardioprotection compared with propofol warrants future investigation.

Conclusion

This study demonstrates that ciprofol protects the myocardium from I/R-induced injury by inhibiting ferroptosis through upregulation of HIF-1α **(Figure 13).** These findings provide a novel mechanistic insight into the potential use of ciprofol for perioperative cardiac protection and support its clinical application in patients at risk of myocardial I/R injury.

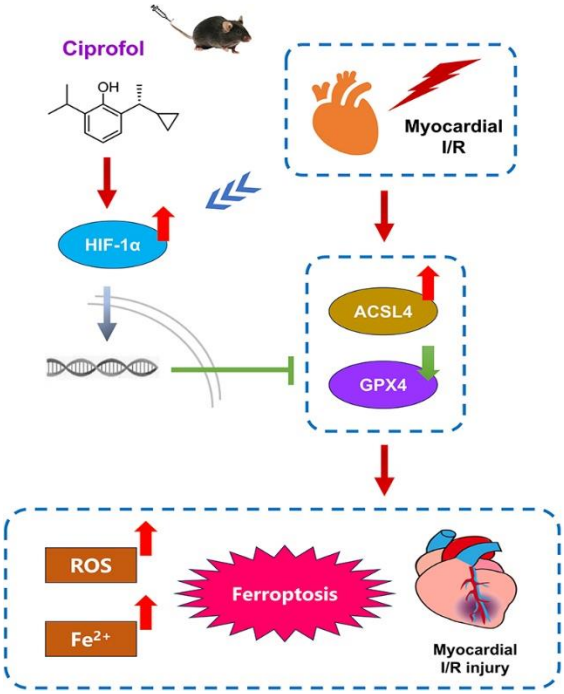

Figure 13. Proposed mechanism illustrating how ciprofol protects mouse hearts from I/R-induced myocardial ferroptosis by enhancing HIF-1α expression.

Acknowledgments: None

Conflict of Interest: None

Financial Support: None

Ethics Statement: None

References

1. Diseases GBD, Injuries C. Global burden of 369 diseases and injuries in 204 countries and territories, 1990-2019: a systematic analysis for the global burden of disease study 2019. Lancet. 2020;396(10258):1204–22. doi:10.1016/S0140-6736(20)30925-9
2. Marijon E, Narayanan K, Smith K, Barra S, Basso C, Blom MT, et al. The Lancet Commission to reduce the global burden of sudden cardiac death: a call for multidisciplinary action. Lancet. 2023;402(10405):883-936. doi:10.1016/S0140-6736(23)00875-9
3. Alexander T, Kumbhani DJ, Mullasari Sankardas A. The future of pharmacoinvasive therapy for st-segment-elevation myocardial infarction reperfusion in the post-STREAM era. Circulation. 2024;149(10):732–3. doi:10.1161/CIRCULATIONAHA.123.066703
4. Del Re DP, Amgalan D, Linkermann A, Liu Q, Kitsis RN. Fundamental mechanisms of regulated cell death and implications for heart disease. Physiol Rev. 2019;99(4):1765–817. doi:10.1152/physrev.00022.2018
5. Zhang Q, Wang L, Wang S, Cheng H, Xu L, Pei G, et al. Signaling pathways and targeted therapy for myocardial infarction. Signal Transduct Target Ther. 2022;7(1):78. doi:10.1038/s41392-022-00925-z
6. Liu S, Bi Y, Han T, Li YE, Wang Q, Wu NN, et al. The E3 ubiquitin ligase MARCH2 protects against myocardial ischemia-reperfusion injury through inhibiting pyroptosis via negative regulation of PGAM5/MAVS/NLRP3 axis. Cell Discov. 2024;10(1):24. doi:10.1038/s41421-023-00622-3
7. Hernandez-Resendiz S, Prakash A, Loo SJ, Semenzato M, Chinda K, Crespo-Avilan GE, et al. Targeting mitochondrial shape: at the heart of cardioprotection. Basic Res Cardiol. 2023;118(1):49. doi:10.1007/s00395-023-01019-9

8. Qin L, Ren L, Wan S, Liu G, Luo X, Liu Z, et al. Design, Synthesis, and Evaluation of Novel 2,6-Disubstituted Phenol Derivatives as General Anesthetics. J Med Chem. 2017;60(9):3606-17. doi:10.1021/acs.jmedchem.7b00254
9. Zhong J, Zhang J, Fan Y, Zhu M, Zhao X, Zuo Z, et al. Efficacy and safety of Ciprofol for procedural sedation and anesthesia in non-operating room settings. J Clin Anesth. 2023;85:111047. doi:10.1016/j.jclinane.2022.111047
10. Wu B, Zhu W, Wang Q, Ren C, Wang L, Xie G. Efficacy and safety of ciprofol-remifentanil versus propofol-remifentanil during fiberoptic bronchoscopy: a prospective, randomized, double-blind, non-inferiority trial. Front Pharmacol. 2022;13:1091579. doi:10.3389/fphar.2022.1091579
11. Liu L, Wang K, Yang Y, Hu M, Chen M, Liu X, et al. Population pharmacokinetic/pharmacodynamic modeling and exposure-response analysis of ciprofol in the induction and maintenance of general anesthesia in patients undergoing elective surgery: a prospective dose optimization study. J Clin Anesth. 2024;92:111317. doi:10.1016/j.jclinane.2023.111317
12. Liu Y, Peng Z, Liu S, Yu X, Zhu D, Zhang L, et al. Efficacy and Safety of Ciprofol Sedation in ICU Patients Undergoing Mechanical Ventilation: a Multicenter, Single-Blind, Randomized, Noninferiority Trial. Crit Care Med. 2023;51(10):1318-27. doi:10.1097/CCM.0000000000005920
13. Sun X, Zhang M, Zhang H, Fei X, Bai G, Li C. Efficacy and safety of ciprofol for long-term sedation in patients receiving mechanical ventilation in ICUs: a prospective, single-center, double-blind, randomized controlled protocol. Front Pharmacol. 2023;14:1235709. doi:10.3389/fphar.2023.1235709
14. Liang P, Dai M, Wang X, Wang D, Yang M, Lin X, et al. Efficacy and safety of ciprofol vs. propofol for the induction and maintenance of general anaesthesia: a multicentre, single-blind, randomised, parallel-group, phase 3 clinical trial. Eur J Anaesthesiol. 2023 ;40(6):399-406. doi:10.1097/EJA.0000000000001799
15. Chen J, Li X, Zhao F, Hu Y. HOTAIR/miR-17-5p axis is involved in the propofol-mediated cardioprotection against ischemia/reperfusion injury. Clin Interv Aging. 2021;16:621–32. doi:10.2147/CIA.S286429
16. Lu Z, Liu Z, Fang B. Propofol protects cardiomyocytes from doxorubicin-induced toxic injury by activating the nuclear factor erythroid 2-related factor 2/glutathione peroxidase 4 signaling pathways. Bioengineered. 2022;13(4):9145–55. doi:10.1080/21655979.2022.2036895
17. Wu X, Li Y, Zhang S, Zhou X. Ferroptosis as a novel therapeutic target for cardiovascular disease. Theranostics. 2021;11(7):3052–9. doi:10.7150/thno.54113
18. Cai W, Liu L, Shi X, Liu Y, Wang J, Fang X, et al. Alox15/15-HpETE Aggravates Myocardial Ischemia-Reperfusion Injury by Promoting Cardiomyocyte Ferroptosis. Circulation. 2023;147(19):1444-60. doi:10.1161/CIRCULATIONAHA.122.060257
19. Ju J, Li XM, Zhao XM, et al. Circular RNA FEACR inhibits ferroptosis and alleviates myocardial ischemia/reperfusion injury by interacting with NAMPT. J Biomed Sci. 2023;30(1):45. doi:10.1186/s12929-023-00927-1
20. Wang Y, Zhang M, Bi R, Su Y, Quan F, Lin Y, et al. ACSL4 deficiency confers protection against ferroptosis-mediated acute kidney injury. Redox Biol. 2022;51:102262. doi:10.1016/j.redox.2022.102262
21. Cao L, Liu J, Ye C, Hu Y, Qin R. Caffeic acid inhibits Staphylococcus aureus-induced endometritis through regulating AMPKalpha/mTOR/HIF-1alpha signalling pathway. J Cell Mol Med. 2024;28(20):70175. doi:10.1111/jcmm.70175
22. Shi J, Song S, Wang Y, Wu K, Liang G, Wang A, et al. Esketamine alleviates ferroptosis-mediated acute lung injury by modulating the HIF-1α/HO-1 pathway. Int Immunopharmacol. 2024;142(Pt A):113065. doi:10.1016/j.intimp.2024.113065
23. Yang X, Wu J, Cheng H, Chen S, Wang J. Dexmedetomidine ameliorates acute brain injury induced by myocardial ischemia-reperfusion via upregulating the Hif-1 pathway. Shock. 2023;60(5):678–87. doi:10.1097/SHK.0000000000002217
24. Miyamoto HD, Ikeda M, Ide T, Tadokoro T, Furusawa S, Abe K, et al. Iron overload via heme degradation in the endoplasmic reticulum triggers ferroptosis in myocardial ischemia-reperfusion injury. JACC Basic Transl Sci. 2022;7(8):800-19. doi:10.1016/j.jacbts.2022.03.012. Erratum in: JACC Basic Transl Sci. 2024;9(1):162. doi:10.1016/j.jacbts.2023.04.001
25. Lei X, Teng W, Fan Y, Zhu Y, Yao L, Li Y, et al. The protective effects of HIF-1α activation on sepsis induced intestinal mucosal barrier injury in rats model of sepsis. PLoS One. 2022;17(5):0268445. doi:10.1371/journal.pone.0268445

26. Du J, Wang C, Chen Y, Zhong L, Liu X, Xue L, et al. Targeted downregulation of HIF-1α for restraining circulating tumor microemboli mediated metastasis. J Control Release. 2022;343:457-68. doi:10.1016/j.jconrel.2022.01.051
27. Qian W, Liu D, Han Y, Liu M, Liu B, Ji Q, et al. Cyclosporine A-loaded apoferritin alleviates myocardial ischemia-reperfusion injury by simultaneously blocking ferroptosis and apoptosis of cardiomyocytes. Acta Biomater. 2023;160:265-80. doi:10.1016/j.actbio.2023.02.025
28. Yan J, Li Z, Liang Y, Yang C, Ou W, Mo H, et al. Fucoxanthin alleviated myocardial ischemia and reperfusion injury through inhibition of ferroptosis via the NRF2 signaling pathway. Food Funct. 2023;14(22):10052-68. doi:10.1039/d3fo02633g
29. Li S, Lei Z, Yang X, Zhao M, Hou Y, Wang D, et al. Propofol Protects Myocardium From Ischemia/Reperfusion Injury by Inhibiting Ferroptosis Through the AKT/p53 Signaling Pathway. Front Pharmacol. 2022;13:841410. doi:10.3389/fphar.2022.841410. Erratum in: Front Pharmacol. 2022;13:910421. doi:10.3389/fphar.2022.910421
30. Knutson AK, Williams AL, Boisvert WA, Shohet RV. HIF in the heart: development, metabolism, ischemia, and atherosclerosis. J Clin Invest. 2021;131(17). doi:10.1172/JCI137557
31. Ge C, Peng Y, Li J, Wang L, Zhu X, Wang N, et al. Hydroxysafflor yellow a alleviates acute myocardial Ischemia/Reperfusion injury in mice by inhibiting ferroptosis via the activation of the HIF-1α/SLC7A11/GPX4 Signaling Pathway. Nutrients. 2023;15(15):3411. doi:10.3390/nu15153411
32. An S, Shi J, Huang J, Li Z, Feng M, Cao G. HIF-1alpha induced by hypoxia promotes peripheral nerve injury recovery through regulating ferroptosis in DRG neuron. Mol Neurobiol. 2024;61(9):6300–11. doi:10.1007/s12035-024-03964-5
33. Chen L, Xie Y, Du X, Qin W, Huang L, Dai J, et al. The Effect of Different Doses of Ciprofol in Patients with Painless Gastrointestinal Endoscopy. Drug Des Devel Ther. 2023;17:1733-40. doi:10.2147/DDDT.S414166
34. Ding YY, Long YQ, Yang HT, Zhuang K, Ji FH, Peng K. Efficacy and safety of ciprofol for general anaesthesia induction in elderly patients undergoing major noncardiac surgery: a randomised controlled pilot trial. Eur J Anaesthesiol. 2022;39(12):960–3. doi:10.1097/EJA.0000000000001759
35. Qin K, Qin WY, Ming SP, Ma XF, Du XK. Effect of ciprofol on induction and maintenance of general anesthesia in patients undergoing kidney transplantation. Eur Rev Med Pharmacol Sci. 2022;26(14):5063–71. doi:10.26355/eurrev_202207_29292
36. Liu X, Ren M, Zhang A, Huang C, Wang J. Nrf2 attenuates oxidative stress to mediate the protective effect of ciprofol against cerebral ischemia-reperfusion injury. Funct Integr Genomics. 2023;23(4):345. doi:10.1007/s10142-023-01273-z
37. Yang Y, Xia Z, Xu C, Zhai C, Yu X, Li S. Ciprofol attenuates the isoproterenol-induced oxidative damage, inflammatory response and cardiomyocyte apoptosis. Front Pharmacol. 2022;13:1037151. doi:10.3389/fphar.2022.1037151
38. Liu Z, Jin Y, Wang L, Huang Z. The effect of ciprofol on postoperative delirium in elderly patients undergoing thoracoscopic surgery for lung cancer: a prospective, randomized, controlled Trial. Drug Des Devel Ther. 2024;18:325–39. doi:10.2147/DDDT.S441950
39. Nair AB, Jacob S. A simple practice guide for dose conversion between animals and human. J Basic Clin Pharm. 2016;7(2):27–31. doi:10.4103/0976-0105.177703
40. Reagan-Shaw S, Nihal M, Ahmad N. Dose translation from animal to human studies revisited. FASEB J. 2008;22(3):659–61. doi:10.1096/fj.07-9574LSF